Electrochemically Synthesized Tin/Lithium Alloy to Convert Laser Light to Extreme Ultraviolet Light

	Nagai Keiji, Musgrave Christopher S. A, Kuwata Naoaki, Kawamura Junichi
journal or publication title	ACS Omega
volume	3
number	10
page range	12422-12427
year	2018-10-02
URL	http://doi.org/10.24517/00067087

Electrochemically Synthesized Tin/Lithium Alloy To Convert Laser Light to Extreme Ultraviolet Light

Keiji Nagai,*,† Christopher S. A. Musgrave,† Naoaki Kuwata,‡ and Junichi Kawamura‡

†Laboratory for Chemistry and Life Science, Institute of Innovative Research, Tokyo Institute of Technology, R1-26, Nagatsuta 4259, Midori-ku, Yokohama 226-8503, Kanagawa, Japan

‡Institute of Multidisciplinary Research for Advanced Materials, Tohoku University, Katahira 2-1-1, Sendai 980-8577, Miyagi, Japan

Ⓢ *Supporting Information*

ABSTRACT: This paper describes lithium−tin alloys as a novel target material to enhance the efficiency of 13.5 nm extreme ultraviolet (EUV) light from generated laser-produced plasmas. Both lithium and tin exhibit EUV emission with the same peak at 13.5 nm. We show that lithium−tin (LiSn) alloys exhibit emission also at 13.5 nm and a mixture of tin and lithium emission by illuminating Nd:YAG laser (1 ns, 2.5 × 10^10, 7.1 × 10^10 W/cm²). The emission spectra and emission angular distribution by using phosphor imaging plates were analyzed to obtain the conversion efficiency from laser light to 13.5 nm light. The Li−Sn alloys were slightly higher than planar tin and between tin and lithium. It would be due to the suppression of self-absorption of 13.5 nm light by the tin plasma.
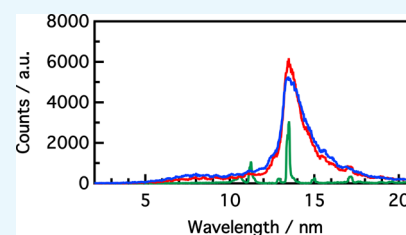
INTRODUCTION

Extreme ultraviolet (EUV) is a promising shorter wavelength light source than the ArF laser (193 nm) in the present semiconductor-integrated circuit manufacturing industry. EUV lithography is at the stage of test for mass production manufacturing a feature size of sub-10 nm.[1,2] The light source of 13.5 nm is one of the critical issues for practical EUV lithography. The most promising EUV source is based on laser-produced plasmas (LPPs) from tin droplets with double pulse laser illumination.[3,4] The target choice of tin,[3−29] especially low-density tin,[19−29] is due to the highest conversion efficiency (CE) from laser light to EUV.[3−5] This is attributed to the unresolved transition array (UTA) arising from Sn^{8+} to Sn^{21+} 4d−4f transitions.[6] The double pulse scheme controls the plasma density to be 10^{-18} atom/cm³ and reduces the amount of debris. According to the theoretical study,[5] the target is expanded to form quasi-steady state within 100 ps, and laser is absorbed almost 100% at the Sn ion density of 10^{10}/cm³, which is 10 mm from the solid tin surface.

On the other hand, lithium LPPs have a simple line emission and an intense line at 13.5 nm that is based on the 1s−2p Lyman a transition in excited Li^{2+} ions, where the electron temperature is 15−18 eV.[30−36] The ionization energy of the lithium ion is much smaller than that of tin. This means that the absorption energy is much less wasted in the lithium LPP compared to Sn LPPs. To increase the lower CE of Li LPP, a forced recombination method was invented,[30−36] where Li^{3+} ions were cooled by low-temperature electrons from a reflector and converted to excited Li^+ ions. In view of the CE depending on different LPP temperatures for Sn and Li, a combination of Sn and Li might serve as an efficient target, that is, Sn should be heated by a laser and Li is heated by the remnant thermal energy of the Sn ions. The hybrid material of tin/lithium is

interesting; however, lithium is air- and moisture-sensitive to serve as a laser target.[37] In this study, we introduce an electrochemically synthesized alloy target and EUV generation from it. The search for such materials is still important for a laboratory-scale and compact EUV source (10−100 Hz), because the present source for lithography becomes huge (>200 W, 100 kHz) and expensive for the laboratory use. For fundamental research, a compact EUV source is still required by combining the relatively small laser and new efficient target materials.

Tin/lithium alloys have been investigated in the field of lithium-ion battery anodes. Tin is of interest as a lithium-ion battery anode material because of its high theoretical specific capacity (993 mA h/g for $Li_{22}Sn_5$), nontoxicity, and low cost, as with other group 14 elements.[38,39] The alloying and dealloying of tin with lithium is possible with the electrochemical technique using thin-film tin electrodes. The composition of the tin/lithium alloy is controlled by the potential of the cell using tin and lithium as the electrode materials.

This paper demonstrates the character of a lithium−tin alloy for generation of EUV at 13.5 nm. Two different alloys were prepared and examined from their EUV spectra and phosphor-imaging plate (IP) data to obtain the CE values.

EXPERIMENTAL SECTION

The Sn thin films were prepared on Cu foil (Nilaco Corp.) substrates by pulsed laser deposition using fourth harmonics of Nd:YAG laser (Quanta-Ray Lab-150-10, Spectra-Physics),

where the substrate was kept at room temperature under vacuum condition of 10^{-4} Pa. The thickness of the Sn films is 2 μm. The stainless-steel electrochemical cell was used for alloying of the Sn with Li. The electrochemical cell was prepared using a Li metal foil as a counter electrode and 1 mol/L LiPF$_6$ solution in 1:1 volume ratio of ethylene carbonate and dimethyl carbonate as the electrolyte. The electrochemical cell was cycled two times by constant current discharge/charge (current density: 67 μA/cm^2) using a potentiostat/galvanostat (VMP3, Bio-Logic). The potential range is between 0.8 and 0.2 V versus Li/Li$^+$. After constant current measurement, the potential was kept for 2.0 V to obtain the Li$_{0.2}$Sn alloy (Li−Sn 43) and kept for 0.4 V to obtain the Li$_{2.5}$Sn alloy (Li−Sn 44).

EUV generation was performed using the same instrumentation setup as shown in Figure 1. We used an Nd:YAG laser

Figure 1. Schematic diagram of the experimental setup to obtain EUV and IP data. A load-lock system was used to insert targets/IPs into the chamber under vacuum conditions. This allowed for quick insertion and removal of the IPs. The distance from the target to the IP was equidistant at all observed angles. The GIS and entrance aperture were 45° with respect to the target.

with 1 ns pulse duration, 2 mJ pulse power (Hamamatsu L11038-01), and a spot size of either 100 or 60 μm, full width half-maximum, to give an intensity of 2.5×10^{10} or 7.1×10^{10} W/cm^2. BAS-TR (Fujifilm, Japan) IPs fitted with a 100 nm thick Zr filter (NTT, Japan) were used to obtain EUV angular distribution data (20°−90°). The Li−Sn targets and reference metals [Li (Kanto Chemical Co.), Japan] and [Sn (Nilaco, Japan)] were ablated as planar materials. Furthermore, all EUV spectra were obtained using a charged couple device set at 45° with respect to the target. An energy calorimeter (Nova II, Ophir) was used to obtain the emission energy, and was set at 45° with respect to target normal and 270 mm distance. Igor Pro software was used for EUV spectra and data analysis.

■ RESULTS

The pulse laser deposition of tin on copper was successfully done, and the X-ray diffraction (XRD) pattern of the Sn film on the Cu substrate is shown in Figure S1, indicating that crystalline Sn is confirmed without any impurities.

Figure 2 shows the constant current discharge/charge voltage profile of Sn film plotted as a function of time. The discharge process from 0 to 1.7 h corresponds the alloying process of Li−Sn. The alloying process of Sn with Li occurs in the plateau region below 0.7 V. In the voltage between 1.5 and 1.2 V, there is a decomposition reaction of the electrolyte due

Figure 2. Constant current (67 μA/cm^2) discharge/charge voltage (vs Li/Li$^+$) profile of Sn film plotted as a function of time.

to the catalytic action of Sn. While the charge process from 1.7 to 1.9 h corresponds to the dealloying of Li−Sn. Reversible reaction of Li−Sn alloying/dealloying is confirmed. After the constant current cycles, the voltage is kept at the each voltage to obtain the different Li−Sn alloy composition.

The EUV emission spectra of reference Sn, reference Li, and Li−Sn alloys can be seen in Figures 3−6, and the 2% band ratios at 13.5 nm per 10−20 nm emission are shown in Table 1.

Figure 3. EUV spectra from tin for the first (blue) and the second (red) shots with a laser intensity of 2.5×10^{10} W/cm^2.

Figure 4. EUV spectra from lithium for the first (blue) and the second (red) shots with a laser intensity of 2.5×10^{10} W/cm^2.

The tin EUV emission spectrum is identical to the previously characterized as an UTA consisting of a strong

Figure 5. EUV spectra for Li−Sn 43 from the first (green) and the second (red) ablated with a laser intensity of 2.5×10^{10} W/cm^2.
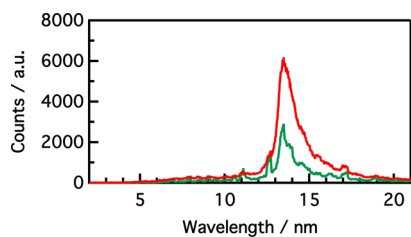
Figure 6. EUV spectra for Li−Sn 44 from the first (green) and the second (red) ablated with a laser intensity of 2.5×10^{10} W/cm^2.

Table 1. EUV Emission in 2% Band Ratio at 13.5 nm per 10−20 nm Range and IP Fitting Values of cos^x θ for Tin, Lithium, and Li−Sn Alloy Materials, for the First and Second Shot

sample/material	2% band ratio at 13.5 nm per 10−20 nm range		x value for cos^x θ		$[I(90) - I(0)]/I(0)$	
	1st	2nd	1st	2nd	1st	2nd
Sn	0.198	0.158	0.41	0.62	0	1.12
Li	0.042	0.047	0.35	0.39	0	0
Li−Sn 43	0.173	0.213	0.25	0.46	0	0.13
Li−Sn 44	0.216	0.221	0.23	0.36	0	0

peak at around 13.5 nm arising from Sn^{8+} to Sn^{21+} 4d−4f transitions[5] for Nd:YAG lasers with intensities in the region of 10^{10} W/cm.[26] The EUV spectrum from the lithium plasma has been characterized as line emission arising from Li^{2+} 1s−2p (13.5 nm), Li^{2+} 1s−3p (11.35 nm), and Li^{1+} 1s^2−4p (17.5 nm).[30] The remaining lines can be attributed to surface impurities, consisting of carbon and oxygen, during sample preparation. All of the Li−Sn EUV emission spectra can be described in the following two manners for both the first and second shots (Table 2); tin-like (Sn-like) emission or lithium-

Table 2. CE Data for tin, Lithium, and Li−Sn Alloys^a

sample/material	CE (%)	
Sn	0.70^b	1.35^c
Li	0.02^b	0.04^b
Li−Sn 43	0.35^b	1.36^c
Li−Sn 44	0.64^b	1.45^c

^{a}For the Li−Sn alloys, the values represent the CE from the surface and cavity, respectively. ^{b}From the first shot. ^{c}From the second shot.

like (Li-like) emission, where the appearance of the EUV emission spectrum was more characteristic of one of the reference metals. Sn-like emission was characterized by a broad UTA around 13.5 nm, and a Li-like emission was represented by line emissions at 11.35 and 13.5 nm. For the first shot, emission from Li−Sn 44 contains more Sn contribution than Li−Sn 43. For the second shot, both of the alloys exhibited stronger emission than those of the first shot, and only a small difference between the two alloys.

The IP response for 10−20 nm EUV was detected after passing through Zr filter. The angular distribution of emission is informative for the absorption (opacity) effect by the plume plasma. Equation 1 is a conventional phomenal analysis of the angular distribution.[7,8]

$$I(\theta) = [I(0) - I(90)]\cos^x \theta + I(90) \qquad (1)$$

where $I(\theta)$ is the intensity at θ degree.

The angular distribution is required to obtain CE from laser energy as estimated by eq 2.

$$CE = \int_0^{2\pi} \int_0^{\pi/2} I(\Theta) E_{cal}(45)/I(45) \, d\Theta \, d\Omega \qquad (2)$$

where $E(45)$, $I(45)$, and LE, are energy at 45°, IP signal at 45°, and irradiated laser energy, respectively. The $E(45)$ value was registered by the calorimeter to be 4.0×10^{-5} J/sr, according to the same condition as the previous research for tin targets,[40] where the ratio of inband (10−20 nm) per out band (longer than 20 nm) emission was 1:1.8.[10]

The CE values for the reference metals were 1.35 and 0.04% for Sn and Li, respectively, for the second shots. For the alloys, the CEs were 1.36 and 1.45% for Li−Sn 43 and Li−Sn 44, respectively, for the second shots. For all of the materials, the first shot exhibited a smaller CE than the second shot, mainly because of the surface contamination.

We measured 2.8 times focused laser illumination (7.1×10^{10} W/cm^2) as shown in Figures S2 and S3, by the use of the same laser and just changing the focus spot. The EUV intensity at 13.5 nm was slightly higher than the case described above, meaning that the present laser intensity is almost optimum to obtain the highest CE. In the case of smaller laser spot size, the error range becomes higher than that for larger spot size and more difficult to control target position.

■ DISCUSSION

Before we discuss the material-dependent EUV emission, we will summarize the first and the second shots. In the previous study for Sn, the difference was observed mainly for the first and later shots, the third and fourth shots gave almost the same data as the second,[40] and then, we focus on the second shots in the present study. As for the alloy sample, the thickness is only 2 μm, and the third shot will reach to the Cu substrate. All of the first shots exhibited weaker emission than those of the second shot and include emissions at 12.9 and 17.3 nm, which are due to O^{5+} (2p−4d) and (2p−3d), respectively. The existence of O atoms means the contamination on the surface by mainly oxidation of the metal and adsorbed water. In the case of the alloy, the contribution of tin was smaller than those of the second shot. It may consist of oxygen impurity is mainly due to lithium oxidation. For the angular distribution shown in Figure 7 and Table 1, we can indicate that the first shots tend to lower uniformity, while the detailed discussion would be complicated because of the surface contamination.

It was expected that a eutectic alloy would show emission properties from both atoms of tin and lithium. Actually, the alloys exhibited emission spectrum of both tin and lithium. The angular distribution parameter of x value in cos^x θ is also between tin and lithium. However, the CE value of the alloy is not middle and slightly higher than that of tin. When we compare the peak of the spectrum at 13.5 nm, the alloy exhibited a sharper peak than that of tin. Such a narrow and relatively monochromatic Sn emission is typically observed for low-density tin targets. The slightly higher CE value could be due to both line emission from lithium and low-density tin effects.

The content of lithium and tin in each alloy would have an effect on the CE (the CE of both Li−Sn alloys: 1.68 and 1.79%). It is interesting that the difference is small in comparison to the one-order difference of lithium content to be Li$_{0.2}$Sn and Li$_{2.5}$Sn for Li−Sn 43 and Li−Sn 44, respectively.
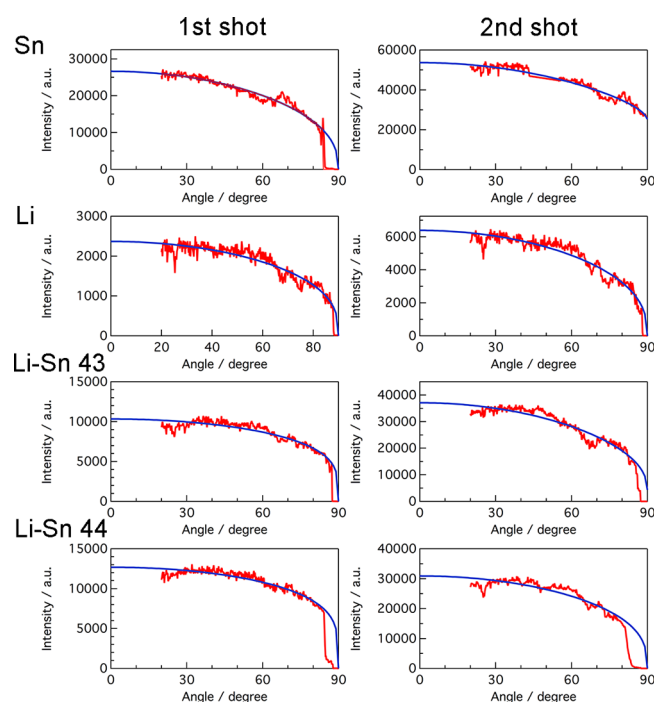
Figure 7. IP data of Sn, Li, and Li−Sn alloys. The data consist of a photoluminescence image (red) and corresponding fitted data (blue) for the first (left) and second (right) shots for each material.

According to the in situ XRD study of tin electrodes for lithium ion batteries, $Li_{0.2}Sn$ has two phases of Sn and Li_2Sn_5 and $Li_{2.5}Sn$ has two phases of β-LiSn and $Li_{22}Sn_5$. These alloys, Li_2Sn_5, β-LiSn, and $Li_{22}Sn_5$ phases, that form as the white tin is lithiated have additional volume ratios of 19, 50, and 280%.[30] From these values, the volume percentages for lithium can be estimated to be 9.5 and 179% per Sn for $Li_{0.2}Sn$ and $Li_{2.5}Sn$, respectively. The theoretical study showed the optimized tin density for highest CE is 10^{-3} order to the solid tin density.[3−5] The present two eutectic alloys have $>10^{-1}$ density, and then, the difference would not so large apparently, while a slight increase in Li−Sn 44 was observed as lower tin density. In the chemical synthesis, the ratio of $Li_{2.5}Sn$ is considerably large, and the present electrochemical method is useful to obtain a compound with such a ratio as theoretically high specific capacity.[38,39] Actually, the previous synthesis based on the porous tin template technique did not show EUV emission,[37] may be due to 100 nm scale heterogeneous mixture, not compound. Then, the present electrochemical synthesis is the first example to exhibit enhancement to combine lithium and tin.

The IP data of the alloys provided an insight into the optical thickness of the generated tin plasmas, because tin plasma shows more re-absorption effect than lithium.[41,42] Both Li−Sn alloy IP data were fit with a $\cos^x \theta$ value, were $x = 0.36$ and 0.46, which are more than that for tin (0.62), implying the suppression of absorption by tin plasma.

Recent photochemistry shows surface-selective carbon oxidation by the use of 13.5 nm light,[43] and the photoresist material is still under investigation.[44] The present target would be a candidate as a compact light source with 10−100 Hz laser for 13.5 nm by combining a conventional millijoule-class laser.

CONCLUSIONS

In this paper, we showed that an EUV light generation from LPP for electrochemically synthesized Li−Sn alloy. It was enhanced EUV light rather than pure Sn, not between of tin and lithium, while the spectra were of those from tin and lithium. The eutectic Li−Sn alloy had an angular distribution between that of tin and lithium, which was indicated by the high-space-resolution IP data. The CE enhancement could be a result of the alloy structure, with Li atoms mixed with Sn to reduce the opacity of the plasma.

ASSOCIATED CONTENT

Ⓢ Supporting Information

The Supporting Information is available free of charge on the ACS Publications website at DOI: 10.1021/acsomega.8b01220.

XRD pattern of the Sn film deposited on the Cu substrate by PLD and EUV spectra of Li and Sn ablated with a laser intensity of 7.1×10^{10} W/cm^2 (PDF)

AUTHOR INFORMATION

Corresponding Author

*E-mail: nagai.k.ae@m.titech.ac.jp.

ORCID Ⓞ

Keiji Nagai: 0000-0002-7641-562X

Notes

The authors declare no competing financial interest.

ACKNOWLEDGMENTS

REFERENCES

(1) Bakshi, V. *EUV Source for lithography*; SPIE: Washington, 2006.

(2) Ito, T.; Okazaki, S. Pushing the limits of Lithography. *Nature* **2000**, *406*, 1027−1031.

(3) Sato, Y.; Tomita, K.; Tsukiyama, S.; Eguchi, T.; Uchino, K.; Kouge, K.; Tomuro, H.; Yanagida, T.; Wada, Y.; Kunishima, M.; Kodama, T.; Mizoguchi, H. Spatial profiles of electron density, electron temperature, average ionic charge, and EUV emission of laser-produced Sn plasmas for EUV lithography. *Jpn. J. Appl. Phys.* **2017**, *56*, 036201.

(4) Tomita, K.; Sato, Y.; Tsukiyama, S.; Eguchi, T.; Uchino, K.; Kouge, K.; Tomuro, H.; Yanagida, T.; Wada, Y.; Kunishima, M.; Soumagne, G.; Kodama, T.; Mizoguchi, H.; Sunahara, A.; Nishihara, K. Time-resolved two-dimensional profiles of electron density and temperature of laser-produced tin plasmas for extreme-ultraviolet lithography light source. *Sci. Rep.* **2017**, *7*, 12328.

(5) Nishihara, K.; Sunahara, A.; Sasaki, A.; Nunami, M.; Tanuma, H.; Fujioka, S.; Shimada, Y.; Fujima, K.; Furukawa, H.; Kato, T.; Koike, F.; More, R.; Murakami, M.; Nishikawa, T.; Zhakhovskii, V.; Gamata, K.; Takata, A.; Ueda, H.; Nishimura, H.; Izawa, Y.; Miyanaga, N.; Mima, K. Plasma physics and radiation hydrodynamics in developing an extreme ultraviolet light source for lithography. *Phys. Plasmas* **2008**, *15*, 056708.

(6) Shimada, Y.; Nishimura, H.; Nakai, M.; Hashimoto, K.; Yamaura, M.; Tao, Y.; Shigemori, K.; Okuno, T.; Nishihara, K.; Kawamura, T.; Sunahara, A.; Nishikawa, T.; Sasaki, A.; Nagai, K.; Norimatsu, T.; Fujioka, S.; Uchida, S.; Miyanaga, N.; Izawa, Y.; Yamanaka, C. Characterization of extreme ultraviolet emission from

laser-produced spherical tin plasma generated with multiple laser beams. *Appl. Phys. Lett.* **2005**, *86*, 051501.

(7) Tao, Y.; Sohbatzadeh, F.; Nishimura, H.; Matsui, R.; Hibino, T.; Okuno, T.; Fujioka, S.; Nagai, K.; Norimatsu, T.; Nishihara, K.; Miyanaga, N.; Izawa, Y.; Sunahara, A.; Kawamura, T. Monochromatic imaging and angular distribution measurements of extreme ultraviolet light from laser-produced Sn and SnO2 plasmas. *Appl. Phys. Lett.* **2004**, *85*, 1919−1921.

(8) Yamaura, M.; Uchida, S.; Sunahara, A.; Shimada, Y.; Nishimura, H.; Fujioka, S.; Okuno, T.; Hashimoto, K.; Nagai, K.; Norimatsu, T.; Nishihara, K.; Miyanga, N.; Izawa, Y.; Yamanaka, C. Characterization of extreme ultraviolet emission using the fourth harmonic of a Nd:YAG laser. *Appl. Phys. Lett.* **2005**, *86*, 181107.

(9) Harilal, S. S. Influence of spot size on propagation dynamics of laser-produced tin plasma. *J. Appl. Phys.* **2007**, *102*, 123306.

(10) Yuspeh, S.; Tao, Y.; Burdt, R. A.; Tillack, M. S.; Ueno, Y.; Najmabadi, F. Dynamics of laser-produced Sn microplasma for a high-brightness extreme ultraviolet light source. *Appl. Phys. Lett.* **2011**, *98*, 201501.

(11) Hayden, P.; Cummings, A.; Murphy, N.; O'Sullivan, G.; Sheridan, P.; White, J.; Dunne, P. 13.5nm extreme ultraviolet emission from tin based laser produced plasma sources. *J. Appl. Phys.* **2006**, *99*, 093302.

(12) Kim, S.-S.; Chalykh, R.; Kim, H.; Lee, S.; Park, C.; Hwang, M.; Park, J.-O.; Park, J.; Kim, H.; Jeon, J.; Kim, I.; Lee, D.; Na, J.; Kim, J.; Lee, S.; Kim, H.; Nam, S.-W. Progress in EUV lithography toward manufacturing. *Proc. SPIE* **2017**, *10143*, 1014306.

(13) Tanaka, H.; Matsumoto, A.; Akinaga, K.; Takahashi, A.; Okada, T. Comparative study on emission characteristics of extreme ultraviolet radiation from CO2 and Nd:YAG laser-produced tin plasmas. *Appl. Phys. Lett.* **2005**, *87*, 041503.

(14) Ueno, Y.; Soumagne, G.; Sumitani, A.; Endo, A.; Higashiguchi, T. Enhancement of extreme ultraviolet emission from a CO2 laser-produced Sn plasma using a cavity target. *Appl. Phys. Lett.* **2007**, *91*, 231501.

(15) Cummins, T.; O'Gorman, C.; Dunne, P.; Sokell, E.; O'Sullivan, G.; Hayden, P. Colliding laser-produced plasmas as targets for laser-generated extreme ultraviolet sources. *Appl. Phys. Lett.* **2014**, *105*, 044101.

(16) Morris, O.; O'Reilly, F.; Dunne, P.; Hayden, P. Angular emission and self-absorption studies of a tin laser produced plasma extreme ultraviolet source between 10 and 18nm. *Appl. Phys. Lett.* **2008**, *92*, 231503.

(17) Hayden, P.; Cummings, A.; Murphy, N.; O'Sullivan, G.; Sheridan, P.; White, J.; Dunne, P. 13.5nm extreme ultraviolet emission from tin based laser produced plasma sources. *J. Appl. Phys.* **2006**, *99*, 093302.

(18) Nagai, K.; Gu, Q.; Yasuda, Y.; Norimatsu, T.; Fujioka, S.; Nishimura, H.; Miyanaga, N.; Izawa, Y.; Mima, K. Oriented and low-density tin dioxide film by sol-gel mineralizing tin-contained hydroxypropyl cellulose lyotropic liquid crystal for laser-induced extreme ultraviolet emission. *J. Polym. Sci., Part A: Polym. Chem.* **2009**, *47*, 4566−4576.

(19) Pan, C.; Gu, Z.-Z.; Nagai, K.; Shimada, Y.; Hashimoto, K.; Birou, T.; Norimatsu, T. SnO2 target with controllable microstructure and thickness for generating extreme ultraviolet light. *J. Appl. Phys.* **2006**, *100*, 016104.

(20) Nagai, K.; Gu, Q.; Gu, Z.; Okuno, T.; Fujioka, S.; Nishimura, H.; Tao, Y.; Yasuda, Y.; Nakai, M.; Norimatsu, T.; Shimada, Y.; Yamaura, M.; Yoshida, H.; Nakatsuka, M.; Miyanaga, N.; Nishihara, K.; Izawa, Y. Angular distribution control of extreme ultraviolet radiation from laser-produced plasma by manipulating the nanostructure of low-density SnO2 targets. *Appl. Phys. Lett.* **2006**, *88*, 094102.

(21) Nagai, K.; Wada, D.; Nakai, M.; Norimatsu, T. Electrochemical fabrication of low density metal foam with mono-dispersed-sized micro- and submicro-meter pore. *Fusion Sci. Technol.* **2006**, *49*, 686−690.

(22) Ge, L.; Nagai, K.; Gu, Z.; Shimada, Y.; Nishimura, H.; Miyanaga, N.; Izawa, Y.; Mima, K.; Norimatsu, T. Dry Tin Dioxide

Hollow Microshells and Extreme Ultraviolet Radiation Induced by CO2Laser Illumination. *Langmuir* **2008**, *24*, 10402−10406.

(23) Choi, I. W.; Daido, H.; Yamagami, S.; Nagai, K.; Norimatsu, T.; Takabe, H.; Suzuki, M.; Nakayama, T.; Matsui, T. Detailed space-resolved characterization of a laser-plasma soft-x-ray source at 135-nm wavelength with tin and its oxides. *J. Opt. Soc. Am. B* **2000**, *17*, 1616−1625.

(24) Okuno, T.; Fujioka, S.; Nishimura, H.; Tao, Y.; Nagai, K.; Gu, Q.; Ueda, N.; Ando, T.; Nishihara, K.; Norimatsu, T.; Miyanaga, N.; Izawa, Y.; Mima, K.; Sunahara, A.; Furukawa, H.; Sasaki, A. Low-density tin targets for efficient extreme ultraviolet light emission from laser-produced plasmas. *Appl. Phys. Lett.* **2006**, *88*, 161501.

(25) Higashiguchi, T.; Hamada, M.; Kubodera, S. Development of a liquid tin microjet target for an efficient laser-produced plasma extreme ultraviolet source. *Rev. Sci. Instrum.* **2007**, *78*, 036106.

(26) Khalenkov, A. M.; Borisenko, N. G.; Kondrashov, V. N.; Merkuliev, Y. A.; Limpouch, J.; Pimenov, V. G. Experience of micro-heterogeneous target fabrication to study energy transport in plasma near critical density. *Laser Part. Beams* **2006**, *24*, 283−290.

(27) Nagai, K.; Nishimura, H.; Okuno, T.; Hibino, T.; Matsui, R.; Tao, Y. Z.; Nakai, M.; Norimatsu, T.; Miyanaga, N.; Nishihara, K.; Izawa, Y. Nanoporous and low-density materials for laser produced extreme UV light source. *Trans. Mater. Res. Soc. Jpn.* **2004**, *29*, 943−946.

(28) Nagai, K. Nanomaterials to generate extreme ultraviolet (EUV) light. In *Encyclopedia of Nanoscience and Nanotechnology*, 2nd ed.; Nalwa, E. H., Ed.; American Scientific Publishers: Stevenson Ranch, CA, 2011.

(29) Harilal, S. S.; O'Shay, B.; Tillack, M. S.; Tao, Y.; Paguio, R.; Nikroo, A.; Back, C. A. Spectral control of emissions from tin doped targets for extreme ultraviolet lithography. *J. Phys. D: Appl. Phys.* **2006**, *39*, 484−487.

(30) Nagano, A.; Inoue, T.; Nica, P.-E.; Amano, S.; Miyamoto, S.; Mochizuki, T. Extreme ultraviolet source using a forced recombination process in lithium plasma generated by a pulsed laser. *Appl. Phys. Lett.* **2007**, *90*, 151502.

(31) Nagano, A.; Mochizuki, T.; Miyamoto, S.; Amano, S. Laser Wavelength Dependence of Extreme ultraviolet Light and Particle Emissions from Laser-Produced lithium plasmas. *Appl. Phys. Lett.* **2008**, *93*, 091502.

(32) Nagano, A.; Mochizuki, T.; Miyamoto, S.; Amano, S. Laser Wavelength Dependence of Extreme ultraviolet Light and Particle Emissions from Laser-Produced lithium plasmas. *Appl. Phys. Lett.* **2008**, *93*, 091502.

(33) Shiriever, G.; Mager, S.; Naweed, A.; Angel, A.; Bergman, K.; Lebert, R. Laser-Produced lithium plasma as a narrow band extended ultraviolet radiation source for photoelectron spectroscopy. *Appl. Opt.* **1998**, *37*, 1243.

(34) George, S. A.; Silfvast, W. T.; Takenoshita, K.; Barnath, R. T.; Koay, C.-S.; Shimkaveg, W.; Richardson, M. EUV generation from lithium laser plasma for lithography. *Proceedings of SPIE Emerging Lithography Technologies X*, 2006; Vol. *6151*, p 615143.

(35) George, S. A.; Silfvast, W. T.; Takenoshita, K.; Bernath, R. T.; Koay, C.-S.; Shimkaveg, G.; Richardson, M. C. Comparative extreme ultraviolet emission measurements for lithium and tin laser plasmas. *Opt. Lett.* **2007**, *32*, 997.

(36) Coons, R. W.; Campos, D.; Krank, M.; Harilal, S. S.; Hassanein, A. Comparison of EUV spectrum and ion emission features from laser produced Sn and Li plasmas. *Proceedings of SPIE Extreme Ultraviolet (EUV) Lithography*, 2010; Vol. *7636*, p 763636.

(37) Nagai, K.; Gu, Q.; Norimatsu, T.; Fujioka, S.; Nishimura, H.; Miyanaga, N.; Nishihara, K.; Izawa, Y.; Mima, K. Nano-structured lithium-tin plane fabrication for laser produced plasma and extreme ultraviolet generation. *Laser Part. Beams* **2008**, *26*, 497−501.

(38) Winter, M.; Besenhard, J. O.; Spahr, M. E.; Novák, P. Insertion electrode materials for rechargeable lithium batteries. *Adv. Mater.* **1998**, *10*, 725−763.

(39) Rhodes, K. J.; Meisner, R.; Kirkham, M.; Dudney, N.; Daniel, C. In situ XRD of thin film tin electrodes for lithium ion batteries. *J. Electrochem. Soc.* **2012**, *159*, A294−A299.

(40) Musgrave, C. S. A.; Murakami, T.; Ugomori, T.; Yoshida, K.; Fujioka, S.; Nishimura, H.; Atarashi, H.; Iyoda, T.; Nagai, K. High-space resolution imaging plate analysis of extreme ultraviolet (EUV) light from tin laser-produced plasmas. *Rev. Sci. Instrum.* **2017**, *88*, 033506.

(41) Fujioka, S.; Nishimura, H.; Nishihara, K.; Sasaki, A.; Sunahara, A.; Okuno, T.; Ueda, N.; Ando, T.; Tao, Y.; Shimada, Y.; Hashimoto, K.; Yamaura, M.; Shigemori, K.; Nakai, M.; Nagai, K.; Norimatsu, T.; Nishikawa, T.; Miyanaga, N.; Izawa, Y.; Mima, K. Opacity effect on extreme ultraviolet radiation from laser-produced tin plasmas. *Phys. Rev. Lett.* **2005**, *95*, 235004.

(42) Tao, Y.; Nishimura, H.; Okuno, T.; Fujioka, S.; Ueda, N.; Nakai, M.; Nagai, K.; Norimatsu, T.; Miyanaga, N.; Nishihara, K.; Izawa, Y. Dynamic imaging of 13.5 nm extreme ultraviolet emission from laser-produced Sn plasmas. *Appl. Phys. Lett.* **2005**, *87*, 241502.

(43) Faradzhev, N. S.; Hill, S. B. EUV-induced oxidation of carbon on TiO 2. *Surf. Sci.* **2016**, *652*, 200−205.

(44) Takei, S. Extreme-ultraviolet and electron beam lithography processing using water developable resist material. *Proceedings of SPIE Nanoengineering: Fabrication, Properties, Optics, and Devices XIV*, 2017; Vol. *10354*, p 1035414.